

- Waspaloy gasket preindented to 80  $\mu\text{m}$ . No pressure medium was used. The low deviatoric stress condition inside the gasket hole was monitored by observing the broadening of the ruby peaks as pressure increased. Experiments performed with either methanol-ethanol-water (16:3:1) or silicon oil as the pressure medium yielded essentially the same results.
15. G. J. Piermarini, S. Block, J. D. Barnett, R. A. Forman, *J. Appl. Phys.* **46**, 2774 (1975).
  16. A sample of  $\text{ZrW}_2\text{O}_8$  of about 12  $\text{mm}^3$  was encapsulated into hexagonal boron nitride and put inside a gasket to guarantee quasi-hydrostatic conditions during the experiment. Pressure was calibrated with the fixed points of bismuth [W. F. Sherman and A. A. Stadtmüller, *Experimental Techniques in High Pres-*

- sure Research* (Wiley, New York, 1987), chap. 6]. After compression, the pellet of  $\text{ZrW}_2\text{O}_8$  was carefully ground in an agate mortar to provide a powder sample suitable for x-ray diffractometry.
17. L. G. Khvostantsev, *High Temp. High Pressures* **16**, 165 (1984).
  18. X-ray powder diffraction data for the cubic and amorphous samples of  $\text{ZrW}_2\text{O}_8$  at ambient conditions were obtained with a Siemens D500 diffractometer equipped with Soller slits in the incident beam, a  $1^\circ$  divergence slit, a 0.15-mm receiving slit, and a graphite monochromator in the secondary beam. Data were collected with  $\text{Cu K}\alpha$  radiation, in the angular range from  $10^\circ$  to  $100^\circ$  ( $2\theta$ ), with a step scan of  $0.05^\circ$  and an acquisition time of 2 s by step

- (1 s for the cubic zirconium tungstate sample).
19. A similar mechanism of pressure-induced amorphization can be found in the review by S. M. Sharma and S. K. Sikka [*Prog. Mater. Sci.* **40**, 1 (1996)].
  20. We thank J. Haines from the Laboratoire de Physico-Chimie des Matériaux-CNRS, Meudon (France) for a critical review of the paper and M. Sasso for help with the toroidal chamber. This work was supported by Conselho Nacional de Desenvolvimento Científico e Tecnológico (CNPq), Financiadora de Estudos e Projetos (FINEP), Fundação de Amparo à Pesquisa do Estado do Rio Grande do Sul (FAPERGS), and Perto S.A. (Brazil).

11 December 1997; accepted 17 March 1998

## Self-Trapping of Dark Incoherent Light Beams

Zhigang Chen, Matthew Mitchell, Mordechai Segev, Tamer H. Coskun, Demetrios N. Christodoulides

“Dark beams” are nonuniform optical beams that contain either a one-dimensional (1D) dark stripe or a two-dimensional (2D) dark hole resulting from a phase singularity or an amplitude depression in their optical field. Thus far, self-trapped dark beams (dark solitons) have been observed using coherent light only. Here, self-trapped dark incoherent light beams (self-trapped dark incoherent wavepackets) were observed. Both dark stripes and dark holes nested in a broad partially spatially incoherent wavefront were self-trapped to form dark solitons in a host photorefractive medium. These self-trapped 1D and 2D dark beams induced refractive-index changes akin to planar and circular dielectric waveguides. The experiments introduce the possibility of controlling high-power coherent laser beams with low-power incoherent light sources such as light emitting diodes.

Solitons have been intensively explored in many areas of physics. In optics, a soliton forms when an optical wavepacket (a pulse or a beam) propagates in a nonlinear medium while maintaining a constant shape without broadening. This is due to a balance between dispersion (in time) or diffraction (in space) and nonlinear “lensing” effects. In the spatial domain, self-trapping of a bright (or dark) optical beam can lead to a spatial soliton when the beam diffraction is counteracted by light-induced self-focusing (or self-defocusing). Thus far, self-trapping of dark beams (1), in the form of 1D dark stripes (2–6) or 2D “holes” (7–11), has been observed using spatially coherent light only. Nature, however, is full of incoherent light sources. In fact, most natural sources of electromagnetic radiation emit light that is incoherent either spatially or temporally, or both. Until recently, the commonly held impression was that solitons are exclusively coherent entities. Our group, however, has experimentally demon-

strated that an incoherent light source can excite incoherent bright solitons in a nonlinear photorefractive medium (12, 13). These were the first observations of self-trapped incoherent wavepackets in nature. Incoherent solitons are altogether new entities, because their phase distribution is random. Following the observations of bright incoherent solitons, a natural question arises: Can such incoherent beams also support dark solitons?

On the basis of knowledge of coherent dark solitons (1), one may speculate that the transverse phase also plays a crucial role for incoherent solitons. Fundamental 1D coherent dark solitons require a transverse  $\pi$  phase shift at the center of the dark stripe, whereas an initially uniform transverse phase leads to a Y-junction soliton. Furthermore, 2D coherent dark solitons (vortex solitons) require a helical  $2m\pi$  transverse phase structure ( $m = \text{integer}$ ). Extending the idea of dark coherent solitons to dark incoherent solitons raises several questions. If dark incoherent solitons were to exist, is their phase structure important (as for coherent dark solitons) or irrelevant (as for bright incoherent solitons, upon which the phase is fully random)? And, if the phase does play a role, how can it be “remembered” by these incoherent entities throughout propagation? Altogether, even

though it has been shown both experimentally (12, 13) and theoretically (14–18) that bright incoherent solitons exist, the existence of dark incoherent solitons is not at all clear. However, we found numerically (19) that when a dark stripe-bearing incoherent beam is launched into a noninstantaneous nonlinear medium (a biased photorefractive crystal), the beam undergoes considerable evolution but eventually stabilizes, with some small oscillatory “breathing,” around a self-trapped solution. Surprisingly, we found that a single dark incoherent soliton requires an initial transverse  $\pi$  phase jump and that the dark incoherent soliton is always gray. In addition, in the extreme case of a very broad dark beam, Hasegawa found a closed-form solution for dark incoherent solitons in plasmas (14). These theoretical results, although not providing answers to the questions raised above, do suggest that dark incoherent solitons should exist.

Here, we report the experimental observation of self-trapping of dark partially spatially-incoherent light beams in the form of 1D dark soliton stripes and 2D soliton holes. To our knowledge, this is the first observation of self-trapping of dark incoherent wavepackets in nature.

A spatially incoherent beam is a “speckled” multimode beam of which the instantaneous intensity pattern consists of many speckles that vary randomly in time. Such an incoherent beam cannot self-trap in an instantaneous nonlinearity. If an incoherent beam is launched into an instantaneous nonlinear medium (for example, optical Kerr medium), each speckle forms a small lens and captures a small fraction of the beam, thus completely fragmenting the beam’s envelope. On the other hand, if the nonlinearity is noninstantaneous with a response time that is much longer than the phase fluctuation time across the beam, then the medium responds to the time-averaged envelope and not to the instantaneous “speckles.” Therefore, for an incoherent soliton, a noninstantaneous nonlinearity is required (16). A convenient choice for producing this state is photorefractive materials for which the optical illumination controls the response time of

Z. Chen, M. Mitchell, M. Segev, Electrical Engineering Department and Center for Photonics and Optoelectronic Materials (POEM), Princeton University, Princeton, NJ 08544, USA.

T. H. Coskun and D. N. Christodoulides, Department of Electrical Engineering and Computer Science, Lehigh University, Bethlehem, PA 18015, USA.

the medium (12, 13). We employed the photorefractive self-defocusing nonlinearity (20) associated with screening solitons (6, 20–22), which can be viewed intuitively in the following manner (6). When a beam bearing a dark stripe propagates in a biased photorefractive crystal, the resistivity of the medium in the illuminated regions decreases because of optically excited electrons, whereas the resistivity within the dark stripe remains unaffected. Thus, the voltage applied across the crystal drops primarily in the dark region, leading to a large space-charge field there, which induces a refractive-index change via the electrooptic effect. The polarity of the field is chosen such that the induced index change is positive and has a self-defocusing effect. As a result, the light in the illuminated portions self-defocuses, and this can balance the diffraction of the dark stripe.

In our experiments, we first converted a coherent beam from an Ar ion laser [wavelength ( $\lambda$ ) = 514 nm] into a quasi-monochromatic spatially incoherent light source by passing it through a rotating diffuser (12). The beam was focused by a lens onto the diffuser, and the scattered light from the diffuser was collected by another lens. The rotating diffuser provided random phase fluctuations across the beam, and made the beam partially spatially incoherent. The spatial coherence of this beam is characterized by a finite correlation distance (that is, the average distance across the beam between two phase-correlated points), which can be varied by changing the relative position between the diffuser and the focusing lens and can be estimated from the speckle size measured when the diffuser is stationary. The rotating diffuser introduced a new speckle pattern every  $\sim 1 \mu\text{s}$ , and the response time of our photorefractive crystal (SBN:60) was  $\sim 0.1 \text{ s}$  at an intensity of  $\sim 1 \text{ W/cm}^2$ . In this way, the crystal “sees” a smooth intensity profile rather than a speckled pattern. The experimental setup is similar to that used for coherent dark photorefractive solitons (6). After the rotating diffuser, the soliton-forming beam was reflected from a phase mask (a  $\lambda/4$  step mirror), which generated a dark notch on a

broad partially spatially incoherent background. This incoherent notch-bearing beam propagated along the crystalline  $a$  axis with its polarization parallel to the  $c$  axis; that is, it is extraordinarily polarized, and it is broad enough to cover the entire input face of the crystal. The crystal is 11.7 mm long and 5.3 mm wide parallel to the  $c$ -direction, along which the external voltage is applied. Our configuration employs a large electrooptic coefficient,  $r_{33}$ , which was measured to be 250 pm/V (in a separate interferometric measurement). We used a uniform ordinarily polarized beam from the same laser as background illumination to mimic the natural dark irradiance in the crystal (6). Self-trapping of the dark notch was observed at a proper bias field because of a balance between diffraction and self-defocusing.

Typical experimental results of self-trapping of a 1D dark incoherent beam are shown (Fig. 1). At the crystal input face, the dark notch is  $18 \mu\text{m}$  [full width at half maximum (FWHM)] wide (Fig. 1a), and it diffracts to  $38 \mu\text{m}$  after the 11.7 mm of propagation (Fig. 1b) when no nonlinearity is present. By applying a voltage of  $-440 \text{ V}$  (negative relative to the  $c$  axis), self-trapping of the dark notch to its initial size is achieved (Fig. 1c). The ratio between the intensity of the incoherent notch-bearing beam and that of the background beam is 0.7. For the results shown (Fig. 1), the average speckle size in the input beam is  $\sim 20 \mu\text{m}$ . In agreement with (19), the observed incoherent dark soliton is gray. Thus, unlike coherent dark solitons which can be either black or gray, dark incoherent solitons are always gray ( $\sim 40\%$  grayness in Fig. 1c). Another notable difference between incoherent and coherent dark (or bright) solitons is the nature of the temporal response of the nonlinearity. Coherent spatial solitons can occur in either instantaneous or noninstantaneous nonlinear media, but incoherent spatial solitons require a noninstantaneous response. For example, Fig. 1d shows what happens when the rotation of the diffuser is stopped and the material nonlinearity is allowed to reach steady state. The self-defocusing medium responds to the “instantaneous” (now stationary) speckles, frag-

menting the beam and prohibiting self-trapping of the dark notch.

Self-trapping of an incoherent dark notch critically depends on the degree of coherence. When the beam is more spatially incoherent, the self-trapped notch becomes grayer, and a higher field is needed for trapping. Figure 2 shows how the dark soliton is affected by the coherence of its carrier beam. Figure 2A shows experimental results with a fully coherent dark soliton (with the diffuser removed) in the same system of Fig. 1. The voltage required for trapping is  $-300 \text{ V}$  ( $\sim 30\%$  less than that of Fig. 1), and the self-trapped notch is nearly black (that is, the intensity in the center of the notch is nearly zero). On the other hand, Fig. 2B shows results with an incoherent dark soliton of which the coherence is further decreased from that of Fig. 1 to an average speckle size of  $\sim 10 \mu\text{m}$ . In this case, the voltage required for trapping is  $-650 \text{ V}$  ( $\sim 48\%$  more than that of Fig. 1), and the self-trapped notch exhibits an increased grayness of about 58%. Except for the spatial coherence and trapping voltage, all other experimental conditions are the same in Figs. 1 and 2. Further decrease of the spatial coherence results in a self-trapped notch that is even more gray and requires an even higher voltage (that is, a larger nonlinearity). Finally, we notice that the dark incoherent soliton self-bends. As the spatial coherence decreases, the self-

**Fig. 1.** Self-trapping of a dark stripe carried by a partially spatially incoherent beam. Shown are photographs and beam profiles of (a) the input beam, (b) diffracted output beam, and (c) the self-trapped output beam. The last photograph (d) shows the output beam with the nonlinearity “on” when the diffuser is stationary, illustrating the fragmentation of an incoherent dark stripe in an instantaneous self-defocusing medium.

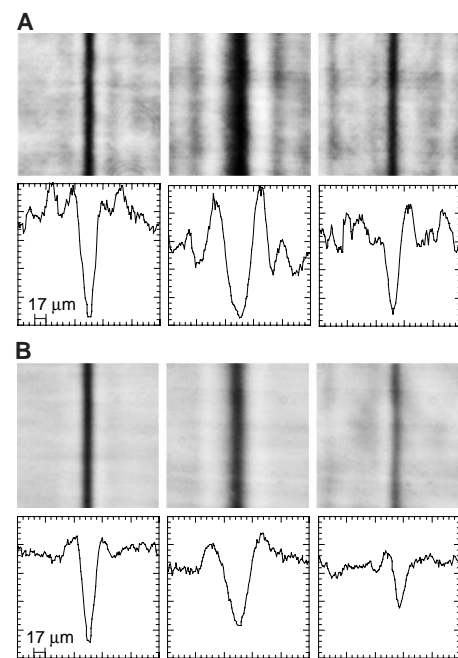
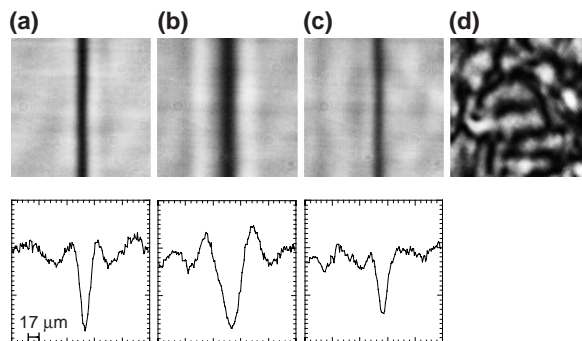


**Fig. 2.** Experimental results showing the effects of beam coherence on self-trapping. (A) and (B) show data similar to Fig. 1, but with different spatial coherence. (A) shows a coherent dark soliton, whereas the coherence in (B) is further reduced from that of Fig. 1.

trapped dark notch self-bends more toward the opposite direction of the crystalline  $c$  axis. For the coherent case (Fig. 2A), no significant bending is observed, whereas for the incoherent case, the dark notch self-bends  $6\ \mu\text{m}$  in Fig. 1 and  $10\ \mu\text{m}$  in Fig. 2B. This increase in self-bending of the self-trapped beam is due to a field-enhanced effect of the diffusion field (23).

We then compared the experimental observations with numerical simulations, employing the method described in (15, 19). We used the experimental crystal parameters, and assumed an input incoherent beam envelope of the hyperbolic tangent type (black and anti-phase) with a dark notch intensity (FWHM) of  $18\ \mu\text{m}$ . We also assumed that the correlation length is initially constant across the input beam. This correlation length is associated with an input angular power spectrum (15, 19) which in this case is assumed to be initially Gaussian. Figure 3A shows the normalized intensity of this input incoherent dark beam (dashed line). The width of the input angular power spectrum is  $0.2^\circ$ , which corresponds to an input correlation length of  $25\ \mu\text{m}$ . After diffraction, the dark notch expands to  $60\ \mu\text{m}$  with 62% grayness (solid line with asterisks). On the other hand, a self-trapped incoherent dark beam (solid line) is established at  $-630\ \text{V}$  and its width is the same as that of the input. Note again that the incoherent dark

soliton is gray and in this case its grayness is 53%. Figure 3B shows the same data when the width of the angular power spectrum is increased to  $0.3^\circ$  (initial correlation length of  $17\ \mu\text{m}$ ). Now the dark beam diffracts to  $90\ \mu\text{m}$  with a grayness of 77% (solid line with asterisks). Self-trapping occurs at  $-1000\ \text{V}$  (solid line) with an output width of  $18\ \mu\text{m}$ . The grayness is now 64%. The results of these simulations are in qualitative agreement with the experimentally observed behavior. The discrepancy between the experiments and these simulations is primarily because, in the experiments, the input beam is never an ideal hyperbolic tangent, as assumed in the calculations.

Finally, we demonstrate self-trapping of an incoherent 2D dark beam. Based on the experience with 2D dark coherent solitons, which are all in the form of vortex solitons (7–11, 24), we launch an incoherent vortex-type beam into our nonlinear crystal. The input vortex beam is generated by replacing the step mirror with a helicoidal phase mask, which creates an optical vortex of unit topological charge (10, 11) that is now nested in a broad spatially incoherent beam. When this incoherent dark beam is propagating through the crystal, it self-traps

in both transverse dimensions at a proper bias field. Figure 4 shows 3D intensity plots and photographs of the input beam, the diffracted output beam, and the self-trapped output beam. This 2D dark incoherent soliton is obtained with an intensity ratio of  $\sim 0.5$  and an applied voltage of  $-550\ \text{V}$ .

As for a 1D dark incoherent soliton, when we decreased the speckle size and made the beam more incoherent, higher trapping voltage was required, and the self-trapped vortex was more gray and less visible (Fig. 5). However, even when the grayness was large (Fig. 5c) and the dark “hole” was almost invisible, we could still monitor its presence: once the vortex was self-trapped and the steady state was reached, we translated the crystal laterally and observed strong guidance of the incoherent beam into the self-trapped channel left by the 2D soliton (Fig. 5d). If we allowed the medium to readjust and reach a new steady state, we retrieved a shifted replica of Fig. 5c, and the guidance at the site of the “old” vortex disappeared. The bright spot in Fig. 5d shows the guidance of the carrier beam as the crystal (and the waveguide induced by the 2D incoherent soliton) is moved to the left, whereas the dark spot is the diffracted “hole” in the beam.

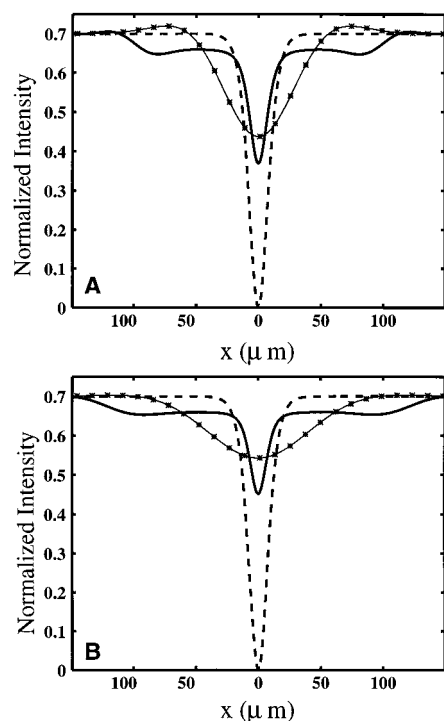


**Fig. 3.** Numerical results showing the intensity profile of the input (dashed curve), diffracted (solid curve with asterisks) and self-trapped (solid curve) incoherent dark beam when the width of the angular power spectrum is (A)  $0.2^\circ$  and (B)  $0.3^\circ$ .

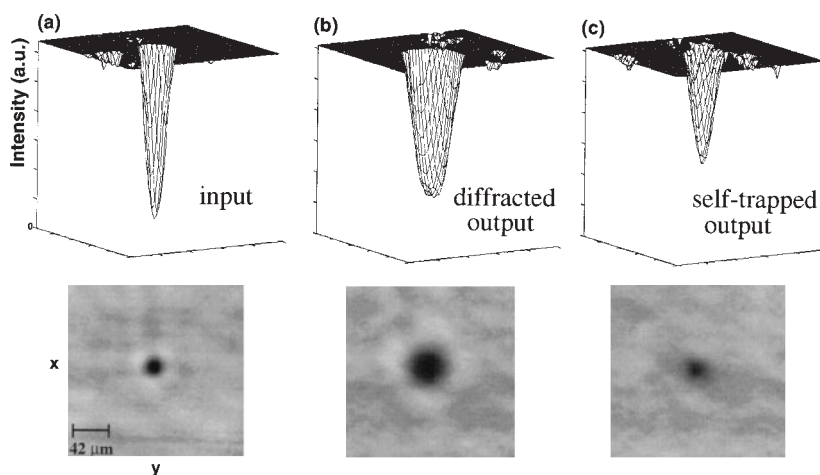


**Fig. 4.** Self-trapping of an optical vortex carried by a partially spatially incoherent beam. Shown are (a) the 3D intensity plots and photographs of the input beam, (b) diffracted output beam, and (c) the self-trapped output beam. For better visualization, the 3D intensity plots have been truncated to remove the noise in the carrier beam.

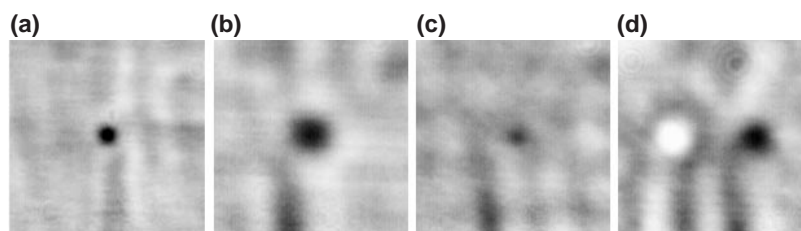


**Fig. 5.** (a) through (c) are the same as in Fig. 4, except that the coherence of the beam is decreased by reducing the speckle size by roughly 50%. The last photograph (d) shows guidance of the carrier beam (bright spot) into the self-trapped channel of the vortex as the crystal is slightly translated to the left.



Having demonstrated dark incoherent solitons, we address several issues. First, from earlier calculations (19) and present experiments we find (within the parameters explored) that the fundamental dark incoherent soliton requires a transverse phase jump (discontinuity) at the center of the dark stripe. How exactly the phase jump survives throughout propagation is still unclear. Second, it is apparent that a different theoretical approach should be pursued to find the stationary dark incoherent soliton solutions and their properties. Such a theory should rely on the modal approach of (16), but incorporate radiation modes as well as multiple guided modes. Therefore, it seems that dark incoherent solitons, or, in a broader sense, self-trapped dark incoherent wavepackets, are fundamentally a new concept: they resemble neither coherent dark solitons nor incoherent bright solitons.

In conclusion, we have demonstrated self-trapping of dark incoherent light beams. Although we employed quasi-monochromatic "partially" spatially incoherent sources, our results suggest that "fully" (spatially and temporally) incoherent dark solitons can be generated using incoherent white-light source. Our results provide direct evidence that a self-trapped incoherent dark beam induces a waveguide that may be used to guide other coherent or incoherent beams. Yet, our observations leave several open questions. For example, how does this incoherent beam maintain the "phase memory" throughout propagation in spite of the random phase fluctuations? Furthermore, our calculations (16, 19) show that the statistics of an incoherent beam are affected by the process of self-trapping. In particular, the coherence length increases in a dark self-trapped beam (inside and close to the dark stripe). This means that dark incoherent solitons can be used for coherence control. It is yet an experimental challenge to actually observe this behavior. We therefore expect that incoherent solitons will bring about new fundamental ideas in nonlinear science. This is especially true because solitons are a universal phenomenon that appears in any nonlinear dispersive system in nature (25).

## REFERENCES AND NOTES

- See review papers by Y. S. Kivshar [*IEEE J. Quantum Electron.* **28**, 250 (1993)] and by Y. S. Kivshar and B. Luther-Davies [*Phys. Rep.* **298**, 81 (1998)].
- G. A. Swartzlander, D. R. Andersen, J. J. Regan, H. Yin, A. E. Kaplan, *Phys. Rev. Lett.* **66**, 1583 (1991).
- G. R. Allan, S. R. Skinner, D. R. Andersen, A. L. Smirl, *Opt. Lett.* **16**, 156 (1991).
- G. Duree *et al.*, *Phys. Rev. Lett.* **74**, 1978 (1995).
- M. D. Iturbe-Castillo, J. J. Sanchez-Mondragon, S. I. Stepanov, M. B. Klein, B. A. Wechsler, *Opt. Comm.* **118**, 515 (1995).
- Z. Chen *et al.*, *Opt. Lett.* **21**, 629 (1996); Z. Chen, M. Segev, S. Singh, T. Coskun, D. N. Christodoulides, *J. Opt. Soc. Am. B* **14**, 1407 (1997).
- G. A. Swartzlander and C. T. Law, *Phys. Rev. Lett.* **69**, 2503 (1992).
- B. Luther-Davies, R. Powles, V. Tikhonenko, *Opt. Lett.* **19**, 1816 (1994).
- A. V. Mamaev, M. Saffman, A. A. Zozulya, *Phys. Rev. Lett.* **78**, 2108 (1997).
- Z. Chen, M. Segev, D. Wilson, R. E. Muller, P. D. Maker, *ibid.*, p. 2948.
- , *Opt. Lett.* **23**, 1751 (1997).
- M. Mitchell, Z. Chen, M. Shih, M. Segev, *Phys. Rev. Lett.* **77**, 490 (1996).
- M. Mitchell and M. Segev, *Nature* **387**, 880 (1997).
- Incoherent solitons were first suggested in plasma physics by A. Hasegawa [*Phys. Fluids* **18**, 77 (1975); **20**, 2155 (1977)], who employed a quasi-particle approach. By averaging over the dynamics of these quasi-particles, a Vlasov transport equation was obtained and solved. Later on, Hasegawa has suggested another technique that further approximates the quasi-particles as plane waves [*Opt. Lett.* **5**, 416 (1980)] and predicted incoherent temporal solitons in multimode optical fibers.
- D. N. Christodoulides, T. Coskun, M. Mitchell, M. Segev, *Phys. Rev. Lett.* **78**, 646 (1997). This coherent density approach is primarily useful to analyze dynamical propagation behavior of arbitrary incoherent beams.
- M. Mitchell, M. Segev, T. Coskun, D. N. Christodoulides, *Phys. Rev. Lett.* **79**, 4990 (1997). This paper provides a modal theory of incoherent bright solitons and finds the soliton solutions, their properties (shape, coherence function), and the range in parameter space that supports them.
- D. N. Christodoulides, T. Coskun, M. Mitchell, M. Segev, *Phys. Rev. Lett.* **80**, 2310 (1998). This paper shows that the coherent density approach and the modal theory developed in (16) are equivalent and complement each other in terms of providing direct information about both the stationary and the dynamic propagation behavior of incoherent bright solitons.
- A. W. Snyder and D. J. Mitchell, *Phys. Rev. Lett.* **80**, 1422 (1998). This work employs a geometrical optics approach for analyzing bright incoherent solitons in the extreme limit of beams that are much larger than their correlation distance.
- T. H. Coskun, D. N. Christodoulides, M. Mitchell, Z. Chen, M. Segev, *Opt. Lett.* **23**, 418 (1998).
- M. Segev, G. C. Valley, B. Crosignani, P. DiPorto, A. Yariv, *Phys. Rev. Lett.* **73**, 3211 (1994); D. N. Christodoulides and M. I. Carvalho, *J. Opt. Soc. Am. B* **12**, 1628 (1995); M. Segev, M. Shih, G. Valley, *ibid.* **13**, 706 (1996).
- The observation of steady-state self-focusing in bi-ased photorefractive crystals was first reported by M. D. Iturbe-Castillo, P. A. Marquez-Aguilar, J. J. Sanchez-Mondragon, S. Stepanov, V. Vysloukh [*Appl. Phys. Lett.* **64**, 408 (1994)].
- The observation of photorefractive screening solitons was first made by M. Shih *et al.*, *Electron. Lett.* **31**, 826 (1995); *Opt. Lett.* **21**, 324 (1996).
- Self-bending of photorefractive screening solitons was first predicted by S. Singh and D. N. Christodoulides [*Opt. Comm.* **118**, 569 (1995)] and first observed with bright solitons in (22). Later on, it was shown [S. Singh, M. I. Carvalho, D. N. Christodoulides, *ibid.* **130**, 288 (1996)] that at large enough applied fields, the self-bending increases with the field.
- A. W. Snyder, L. Polodian, D. J. Mitchell, *Opt. Lett.* **17**, 789 (1992).
- "Solitons are a gift from God. Therefore it is a sin not to use them." A. Hasegawa, at a Colloquium at Princeton University, December 1997.
- Supported by the U.S. Army Research Office, the U.S. Air Force Office of Scientific Research, and NSF.

22 January 1998; accepted 11 March 1998

## Ultrathin Films of a Polyelectrolyte with Layered Architecture

A. R. Esker, C. Mengel, G. Wegner\*

Posttransfer modification of preformed Langmuir-Blodgett films of poly(*tert*-butyl methacrylate) and poly(*tert*-butyl acrylate) by gaseous hydrochloric acid yields films with layered architecture of poly(methacrylic acid) and poly(acrylic acid), respectively. X-ray reflectivity and infrared spectroscopy confirm monolayer by monolayer transfer of the source polymers and their transformation to acid multilayer assemblies with retention of low surface roughnesses. The incorporation of cross-linking groups into the system offers the possibility for further chemical modification to produce ultrathin films of model networks desirable for bioadsorption studies and as hydrophilic spacing layers for tethered membranes.

The Langmuir-Blodgett (LB) technique offers the possibility to fabricate highly ordered films with monolayer by monolayer control of thickness and low surface roughnesses (1). In addition, nearly ideal model surfaces are obtained, the properties of which are controlled by the chemical structure of the last layer in the transfer process. These properties are desirable for a number

of applications such as model surfaces for protein adsorption, modified substrates for supported membranes, and microelectronic and optical devices (2–4). Unfortunately, not all molecules, such as water-soluble polymers, can be processed into single-component multilayers by this technique. Appropriate materials must have the proper balance between hydrophilic and hydrophobic properties and also between rigid (shape-persistent) and flexible moieties to facilitate the formation of a stable, liquid, crystalline-like monolayer phase at the air-water interface (4). This balance is neces-

Max-Planck-Institut für Polymerforschung, Ackermann Weg 10, D-55128 Mainz, Germany.

\*To whom correspondence should be addressed. E-mail: wegner@mpip-mainz.mpg.de